

# Nuclear longitudinal structure function in eA processes at the LHeC

G.R.Boroun,<sup>\*</sup> B.Rezaei,<sup>†</sup> and S.Heidari

*Physics Department, Razi University, Kermanshah 67149, Iran*  
(Dated: March 25, 2018)

The nucleon and nuclear longitudinal structure functions are determined by the Kharzeev-Levin-Nardin (KLN) model of the low  $x$  gluon distribution. The behavior of the gluon distribution ratio  $R_g = G^A/AG^p$  and the ratio  $R_L^{total} = F_L^{A-total}/AF_L^{p-total}$  in this processes are found. The heavy longitudinal structure function ratios in eA processes at the LHeC region are discussed. Heavy contributions to the ratio of the total longitudinal structure function are considerable and should not be neglected especially at smaller  $x$  of the LHeC project. In the KLN model the new geometrical scaling for transition from the linear to nonlinear regions in accordance with the LHeC processes is used, whose results intensively depended on the heavy quarks mass effect.

## I. Introduction

Our knowledge of the gluon distribution function of free nucleons comes from the deep inelastic scattering (DIS) measurements in lepton-nucleon collisions, as at low- $x$  the gluon distributions are predominant at all values of  $Q^2$ . There is a transition from the linear to nonlinear regions as it can be tamed by screening effects. These nonlinear terms reduce the growth of the gluon distribution at low  $x$  values. Therefore DIS processes in LHeC provide very important tools for probing the gluon distribution in the nucleons and nuclei. The nuclear gluon distribution  $xg^A(x, Q^2)$  can be determined from the gluon distribution of nucleons which are bounded in a nucleus. Also, the nuclear distribution functions can be extracted from the measurements of deep inelastic lepton-nucleus scattering (eA processes). In the electron-proton/ion collider LHeC, we intended to demonstrate how the low  $x$  data are possible for nuclear targets and could constrain the nuclear gluon distribution function.

The LHeC shows an increase in the kinematic range of the deep inelastic scattering (DIS) because the DIS kinematics are  $2 < Q^2 < 100,000 \text{ GeV}^2$  and  $0.000002 < x < 0.8$  with a center-of-mass energy of about  $\sqrt{s_{ep}} > 1 \text{ TeV}$ . Clearly this increase in the precision of parton distribution functions (PDF's) at low- $x$  kinematic region is expected to cause by the non-linear effects in the so-called saturation region [1-4]. The nuclear parton distribution functions (nPDF's) can be determined based on the DGLAP [5-6] evolution, analogous to the parton distributions of the free proton. At low  $x$ , the data show a reduction of the nuclear distribution functions with respect to the free distribution functions. This phenomenon is caused by the

nuclear shadowing effects as  $xg^A(x, Q^2) < Axg^N(x, Q^2)$ . These shadowing corrections give rise to nonlinear terms in the evolution equation of the gluon distribution function. Indeed, these behaviors are tamed by the saturation effects. In the gluon saturation approach, an important point is the  $x$ -dependence saturation scale  $Q_s^2(x)$  where it is the critical line between the linear and nonlinear regions. It is expected that the nonlinear effects are small in  $Q^2 > Q_s^2(x)$  and it should be strong in  $Q^2 < Q_s^2(x)$  which generate geometrical scaling in this region. Therefore the nuclear reduced cross section is dependent upon the single variable  $\tau_0 = \frac{Q^2}{Q_s^2(x)}$ , as  $\sigma_{\gamma^*A}(x, Q^2) = \sigma_{\gamma^*A}(\tau_0)$  and the saturation scale is given by  $Q_s^2(x) = Q_0^2(\frac{x}{x_0})^{-\lambda}$  [7-9]. Here  $Q_0^2 = 0.34 \text{ GeV}^2$ ,  $x_0 = 3.0 \times 10^{-3}$  and exponent  $\lambda$  is a dynamical quantity at the order of  $\lambda \simeq 0.25$ .

The paper is organized as follows: Section II deals with KLN model in transition from traditional geometrical scaling to new geometrical scaling with respect to heavy quarks mass. Section III introduces the nuclear longitudinal structure function by considering the heavy quarks portion. In section IV we finalized the total longitudinal structure function calculation for light and heavy nuclei. Finally, in Sec.V we summarized the results.

## II. KLN model and saturation scale

We focused on the nuclear longitudinal structure function based on the geometrical scaling at low  $x$ . The main purpose of this study was to analyze possible compatibility of the new geometrical scaling with the KLN model for transition from the linear to nonlinear nuclear behavior. In heavy production, the geometrical scaling is expected to be violated by heavy quarks mass, since the traditional geometrical scaling ( $\tau_0$ ) can be modified to

<sup>\*</sup>Electronic address: grboroun@gmail.com; boroun@razi.ac.ir

<sup>†</sup>brezaei@razi.ac.ir

take into account heavy quarks mass [9]:

$$\tau_H = (1 + \frac{4m_H^2}{Q^2})^{1+\lambda} \frac{Q^2}{Q_0^2} (\frac{x}{x_0})^\lambda. \quad (1)$$

In the KLN model [10], a simple relation for the unintegrated gluon distribution was observed as it is related to the gluon distribution by the following form

$$G(x, Q^2) = \int^{Q^2} dk_t^2 \varphi(x, k_t^2), \quad (2)$$

where  $\varphi$  is the unintegrated gluon distribution of a nucleon or nucleus. Authors in Ref.[10] used a simplified assumption about the form of  $G(x, Q^2)$  by two regions of integration over  $Q^2$  defined in accordance with the critical line  $Q_s^2$ . For a nucleon we use the KLN Ansatz as

$$G(x, Q^2) = \begin{cases} \frac{K_0 S}{\alpha_s(Q_s^2)} Q^2 (1-x)^4, & Q^2 < Q_s^2 (\tau_0 < 1) \\ \frac{K_0 S}{\alpha_s(Q_s^2)} Q_s^2 (1-x)^4, & Q^2 > Q_s^2 (\tau_0 > 1), \end{cases} \quad (3)$$

where the numerical coefficient  $K_0$  can be determined from the gluon density, which is usually taken from the parameterization groups and  $S$  is the area corresponds to the target. Here the factor  $(1-x)^4$  is to describe the fact that the gluon density is small at high  $x$  values.

The gluon distribution function, for a nucleus with the mass number  $A$ , can be exploited to  $G^A(x, Q^2)$  with replacements  $S \rightarrow S^A = A^{\frac{2}{3}} S$  and  $Q_s^2 \rightarrow Q_s^{2A} = A^{\frac{1}{3}} Q_s^2$  [11]. The gluon distribution for a nucleus with respect to Eq.3 can be written as

$$G^A(x, Q^2) = \begin{cases} \frac{K_0 S^A}{\alpha_s(Q_s^{2A})} Q^2 (1-x)^4, & Q^2 < Q_s^{2A} (\tau_0^A < 1) \\ \frac{K_0 S^A}{\alpha_s(Q_s^{2A})} Q_s^{2A} (1-x)^4, & Q^2 > Q_s^{2A} (\tau_0^A > 1). \end{cases} \quad (4)$$

The transition point between the linear and nonlinear regions in accordance with the critical line for the proton ( $A = 1$ ) and a nucleus ( $A$ ) is

$$x_c = x_0 (\frac{Q_0^2 A^{1/3}}{Q^2})^{1/\lambda}. \quad (5)$$

Table.1 shows that the critical point is dependent on the mass number  $A$  and  $Q^2$  values. At low  $x$  values, the transition point between the linear and nonlinear behavior is observable for light nuclei at low  $Q^2$  and for heavy nuclei at low and moderate  $Q^2$  values in  $eA$  processes. These critical points refer to zero quark mass so that the geometrical scaling defined by  $\tau_0^A (= \frac{Q^2}{Q_s^{2A}(x)})$ . Since mass of heavy quarks in the LHeC region is not negligible, therefore the geometrical scaling is sensitive to the mass of the heavy quarks. This is consistent with a new geometrical scaling  $\tau_H^A$  into the one as follows  $\tau_H^A = (1 + \frac{4m_H^2}{Q^2})^{1+\lambda} \frac{Q^2}{Q_s^{2A}}$ . We expect that the transition points shift to lower  $x$  values as transition between the linear and nonlinear behaviors tamed at low  $x$  values. As to the mass correction,

the critical point is given by the following form

$$x_c = x_0 (\frac{Q_0^2 A^{1/3}}{Q^2 (1 + \frac{4m_H^2}{Q^2})})^{1/\lambda}. \quad (6)$$

In Tables 2-4, we observe the heavy quark mass effects on the critical points. Indeed, the difference between the (traditional) geometrical scaling variable ( $\tau_0$ ) and the "new" geometrical scaling variable ( $\tau_H$ ), particularly for  $eA$  ( $\tau_0^A$  and  $\tau_H^A$ ) is strong dependence on the heavy quark mass as  $\frac{\Delta\tau}{\tau_0}$  or  $\frac{\Delta\tau^A}{\tau_0^A} = (1 + \frac{4m_H^2}{Q^2})^{1+\lambda} - 1$ .

Fig.1 shows the behavior of the ratio  $R_g = \frac{G^A(x, Q^2)}{AG^p(x, Q^2)}$  for light and heavy nuclei  $A = 12$  and  $A = 208$  respectively at  $Q^2$  values of 2, 10 and 100  $GeV^2$  in order to determine the gluon densities in nuclei. The magnitude of shadowing effects are considered by the geometrical scaling behavior at low  $x$  values. We observe the saturation effects for the ratio  $R_g$  at  $x < 10^{-2}$  and for small values of  $Q^2$  at light and heavy nuclei by using the traditional scaling. In Figs.2-3, we observe that the critical points related to the new geometrical scaling are noticeable in a wide region of  $x$  ( $x < 10^{-5}$  upto  $x < 10^{-15}$ ). These observations are essential in determining of these ratios when we take into account the heavy quarks mass effects.

### III. Nuclear longitudinal structure function

Now, we consider the nuclear longitudinal structure function at  $eA$  processes with respect to the nuclear gluon density behavior. The nuclear longitudinal structure function is interested because it is directly sensitive to the nuclear gluon density through the transition  $g^A \rightarrow q^A \bar{q}^A$  in  $eA$ -DIS. Indeed a measurement of  $F_L^A(x, Q^2)$  can be used to extract the nuclear gluon structure function. Therefore the measurement of  $F_L^A$  provides a sensitive test of perturbative QCD (pQCD). Since the longitudinal structure function  $F_L$  contains rather large heavy flavor contributions at small- $x$  region, so the measurements of these observables in the  $eA$  processes have told us about the ratio of the heavy quarks contribution to the nuclear longitudinal structure function and also the dependence of nuclear parton distribution functions (nPDFs) on heavy quarks mass. In perturbative QCD, the nuclear longitudinal structure function can be written as

$$x^{-1} F_L^A = C_{L,ns} \otimes q_{ns}^A + \langle e^2 \rangle (C_{L,q} \otimes q_s^A + C_{L,g} \otimes g^A) + x^{-1} F_L^{Heavy-A}, \quad (7)$$

where the symbol  $\otimes$  indicates convolution over the variable  $x$  as:  $A(x) \otimes B(x) = \int_x^1 \frac{dy}{y} A(y) B(\frac{x}{y})$ . Here  $q_{ns}^A$ ,  $q_i^A$  and  $g^A$  represent the distributions of quarks and gluons in nuclei, respectively.  $\langle e^2 \rangle$  is the average squared

charge ( $= \frac{2}{9}$  for light quarks) and  $C_{L,a}$  is the perturbative expansion of the coefficient functions as it follows

$$C_{L,a}(\alpha_s, x) = \sum_{n=1} \left(\frac{\alpha_s}{4\pi}\right)^n c_{L,a}^{(n)}(x). \quad (8)$$

At low  $x$ , the gluon contribution to the total nuclear longitudinal structure function dominates over the singlet and nonsinglet contributions as

$$F_L^A|_{x \rightarrow 0} \simeq F_L^{g-A} + F_L^{Heavy-A}. \quad (9)$$

The gluonic nuclear longitudinal structure function is given by

$$F_L^{g-A}(x, Q^2) = \sum_{n=1} \left(\frac{\alpha_s}{4\pi}\right)^n \langle e^2 \rangle c_{L,g}^{(n)}(x) \otimes G^A(x, Q^2). \quad (10)$$

The nuclear heavy quark-longitudinal structure function, at low-  $x$ , is depends on the nuclear gluon distribution when neglecting the contributions due to incoming light quarks and anti-quarks in boson gluon fusion processes. Therefore

$$\begin{aligned} F_L^{Heavy-A}(x, Q^2) &= C_{L,g}^{Heavy}(x, Q^2) \otimes G^A(x, Q^2) \\ &\equiv \sum_{n=1} F_L^{(n), Heavy-A}(x, Q^2), \end{aligned} \quad (11)$$

where  $n$  indicates the order of  $\alpha_s$ . At low  $x$  values, Eqs.10 and 11 are explicitly dependent on the strong coupling constant and nuclear gluon density.

Similarly, in the electron-proton collision, the gluonic longitudinal structure function is directly dependent on the gluon distribution function. Some analytical solutions of the Altarelli- Martinelli equations [13] using the expanding method and hard pomeron behavior initialized by Cooper-Sarkar *et al.*, have been reported in last years

[14-15] with considerable phenomenological success.

At leading order (LO) analysis, the gluonic nuclear longitudinal structure function is given by

$$\begin{aligned} F_L^{g-A}(x, Q^2) &= \frac{\alpha_s}{4\pi} \left[ \sum_{i=1}^{N_f} e_i^2 \right] \int_x^1 \frac{dy}{y} [8(x/y)^2(1-x/y)] \\ &\times G^A(y, Q^2), \end{aligned} \quad (12)$$

and

$$\begin{aligned} F_L^{Heavy-A}(x, Q^2) &= F_L^{c-A}(x, Q^2) + F_L^{b-A}(x, Q^2) \\ &+ F_L^{t-A}(x, Q^2), \end{aligned} \quad (13)$$

where

$$\begin{aligned} F_L^{Heavy-A}(x, Q^2, m_H^2) &= 2e_H^2 \frac{\alpha_s(\mu_H^2)}{2\pi} \int_{x_{a_H}}^1 \frac{xdy}{y^2} \\ &\times C_{L,g}^H\left(\frac{x}{y}, \frac{m_H^2}{Q^2}\right) G^A(y, \mu_H^2). \end{aligned} \quad (14)$$

Here  $a_H = 1 + 4\frac{m_H^2}{Q^2}$ ,  $C_{L,g}^H$  is the heavy coefficient function related to the heavy quarks mass. The scale  $\mu_H (= \sqrt{\frac{Q^2}{2} + 4m_H^2})$  is the mass factorization and the renormalization scale, and  $\alpha_s(\mu_H^2)$  is the running coupling constant. The heavy longitudinal coefficient function can be expressed as

$$C_{L,g}^H(z, \zeta) = -4z^2 \zeta_H \ln \frac{1+\beta_H}{1-\beta_H} + 2\beta_H z(1-z), \quad (15)$$

where  $\beta_H^2 = 1 - \frac{4z\zeta_H}{1-z}$  ( $\zeta_H \equiv \frac{m_H^2}{Q^2}$ ).

The low-  $x$  behavior of the nuclear gluon distribution function in accordance with the KLN model can be exploited to the nuclear longitudinal structure function. Therefore  $F_L^{A-total}$  at low  $x$  can be found as

$$\begin{aligned} F_L^{A-total} &= \frac{\alpha_s}{4\pi} \left[ \sum_{i=1}^{N_f} e_i^2 \right] \int_x^1 \frac{dy}{y} [8(x/y)^2(1-x/y)] G^A(y, Q^2) + 2e_c^2 \frac{\alpha_s(\mu_c^2)}{2\pi} \int_{a_{cx}}^1 \frac{xdy}{y^2} C_{L,g}^c\left(\frac{x}{y}, \zeta_c\right) G^A(y, \mu_c^2) \\ &+ 2e_b^2 \frac{\alpha_s(\mu_b^2)}{2\pi} \int_{a_{bx}}^1 \frac{xdy}{y^2} C_{L,g}^b\left(\frac{x}{y}, \zeta_b\right) G^A(y, \mu_b^2) \\ &+ 2e_t^2 \frac{\alpha_s(\mu_t^2)}{2\pi} \int_{a_{tx}}^1 \frac{xdy}{y^2} C_{L,g}^t\left(\frac{x}{y}, \zeta_t\right) G^A(y, \mu_t^2). \end{aligned} \quad (16)$$

The behavior of the ratio  $R_L = \frac{F_L^{g-A}}{AF_L^{g-p}}$  as a function of  $x$  for  $Q^2 = 2, 10$  and  $100 \text{ GeV}^2$  and nuclei  $A = 12$  and  $A = 208$  is presented in Fig.1. The transition point between the linear and nonlinear regions is shown at low

$Q^2$  values in this figure. These results are comparable with EKS [16] and EPS [17] analysis in comparison with DS [18] and HKN [19] parameterizations at low  $x$  and also with nuclear PDFs from the LHeC perspective [20]. The magnitude of the shadowing effect is dependent on

$Q^2$  values and mass number ( $A$ ). In fact, this model predict a large value for the shadowing effects at low and high  $Q^2$  values. The shadowing effects for heavy nuclei are larger than light nuclei at a wide range of  $x$  and  $Q^2$ . Figures 2-3 show the transition point between linear and nonlinear regions with respect to the new geometrical scaling shifted towards very low  $x$  values, and this relates to the nuclear mass in eA processes.

In Figs.4-5, we present the small- $x$  behavior of the ratio  $R_L^H$  in accordance with the traditional transition point (Eq.5) as a function of  $x$  for  $Q^2 = 2, 10$  and  $100 \text{ GeV}^2$  and nuclei  $A = 12$  and  $A = 208$ . In these figures, we observed antishadowing and shadowing behaviors at low  $x$  and low  $Q^2$  values along the traditional geometrical scaling (Eq.5). In the all cases, the depletion and enhancement in these ratios reflect the linear(at  $x > x_c$ )/linear(at  $x > x_c$ ), nonlinear(at  $x < x_c$ )/linear(at  $x > x_c$ ) and nonlinear(at  $x < x_c$ )/nonlinear(at  $x < x_c$ ) behavior for nuclei/nucleon related to Eq.5. The enhancement in the ratio nuclei/nucleon (i.e. antishadowing behavior) is related to the nonlinear behavior of nuclei. This is dependence to the coherent multiple scattering where introduces the medium size enhanced (in powers of  $A^{1/3}$ ) nuclear effects [22]. Indeed nuclear shadowing is controlled by the interplay of photon fluctuations lifetime and coherent time for transition between no shadowing and saturated shadowing at very small  $x$ . The gluon shadowing is negligibly at  $x > 0.01$  which covers the whole range on the NMC data [23]. Indeed transition of nuclei from linear to nonlinear regions is faster than transition of nucleon.

The new transition points for these ratios are shown in figures 6-7. This is consistent with Eq.6 for charm, bottom and top quarks. Indeed the nonlinear effects are predominant for light and heavy nuclei at low-  $Q^2$  values. The shadowing effects for  $A = 12$  are observable at  $Q^2 = 2 \text{ GeV}^2$  and  $x < 10^{-6}$  and for  $A = 208$  are observable at  $Q^2 = 2$  and  $10 \text{ GeV}^2$  at  $x < 10^{-5}$  by the charm content of the nuclei and nucleon. For bottom and top contribution to the longitudinal structure functions, the shadowing effects will be noticeable at  $x < 10^{-7}$  and low  $Q^2$  values, which may be expected to be predict at the LHeC energies. A comparison between  $R_L$ (Fig.1) and  $R_L^H$ (Figs.6-7) shows that transition point for going to the shadowing region is at larger values of  $x$ . This is consistent with light and heavy quarks mass.

#### IV. Total longitudinal structure function

Let us now discuss about the ratio of the total longitudinal structure functions. It is well known that the inclusive observable  $F_L^{total}$  is strongly dependent on the gluon distribution and heavy contributions to the structure function. Fig.8 shows the results of the

total longitudinal structure function ratio for  $A = 12$  and  $A = 208$  at  $Q^2$  value of  $2 \text{ GeV}^2$ , where saturation effect is more observable than other  $Q^2$  values. In this case, the significant nonlinear effect is observable as this effect start to appear at  $x \leq 10^{-3}$  for heavy nuclei and decrease to lower  $x$  values for light nuclei. Therefore the shadowing effect For light and heavy nuclei are observable at low  $x$  values. An enhancement at behavior of the ratio ( $R_L^{total}$ ) for light nuclei (in Fig.8 on the left panel) is due to the KLN gluon model and caused by the anti-shadowing effects. Finally the ratio of the total longitudinal structure function decreases as  $A$  increases.

#### V. Summary

In conclusion, we have observed that the KLN model for the total longitudinal structure function ratio  $R_L^{total}$  gives the saturation effect of the heavy quarks effect to the light flavors at small  $x$ . This ratio shows shadowing effects for heavy nuclei at low  $x$ . But for light nuclei an enhancement in addition to depletion is shown at this region. The results are close to EPS nuclear distribution. Lastly, one important conclusion is that heavy contribution to the total longitudinal structure function ratio  $R_L^{total} = F_L^{A-total}/AF_L^{p-total}$  is considerable and cannot be neglected especially at smaller  $x$  of the LHeC project.

#### Acknowledgments

We thank F.O.Durães for useful discussions, comments and reading the manuscript.

#### REFERENCES

1. LHeC workshops 2015 (<http://cern.ch/lhec>).
2. G.R.Boroun, Phys.Lett.B**744** (2015)142; Phys.Lett.B**741** (2015)197.
3. J.L.Abelleira Fernandez, et.al., [LHeC Collab.], J.Phys.G**39** (2012)075001.
4. M.Klein, Ann.Phys. **528**,No.1-2(2016)138-144.
5. V.N. Gribov and L.N. Lipatov, Sov. J. Nucl. Phys.**18** (1972) 438.
6. L.N. Lipatov, Sov. J. Nucl. Phys.**20** (1975) 93; G. Altarelli and G. Parisi, Nucl. Phys. **B126** (1977) 298; Yu.L. Dokshitzer, Sov. Phys. JETP **46** (1977) 641.
7. M.Praszalowicz and T.Stebel, JHEP **04** (2013) 169.
8. G.Beuf and D.Royon, arXiv:hep-ph/0810.5082(2008).
9. T.Stebel, Phys. Rev. D **88** (2013), 014026.
10. D.Kharzeev, E.Levin and M.Nardi, Nucl.Phys.A**730**

TABLE I: Critical point  $x_c$  along the critical line  $Q_s^2 = Q^2$ .

$Q^2(GeV^2)$	$x_c^{A=1}$	$x_c^{A=12}$	$x_c^{A=208}$
2	0.25E-5	0.70E-4	0.31E-2
10	0.40E-8	0.11E-6	0.50E-5
100	0.40E-12	0.11E-10	0.50E-9

TABLE II: Critical point  $x_c$  with new geometrical scaling to take into account  $m_c$ .

$Q^2(GeV^2)$	$x_c^{A=1}$	$x_c^{A=12}$	$x_c^{A=208}$
2	0.41E-8	0.12E-6	0.51E-5
10	0.50E-9	0.14E-7	0.61E-6
100	0.31E-12	0.85E-11	0.39E-9

(2004)448;Nucl.Phys.A**747** (2005)609.

11. F.Carvalho, F.O.Durães, F.S.Navarra and S.Szpigel, Phys.Rev.C**79** (2009)035211.

12. E.R.Cazaroto, F.Carvalho. V.P.Goncalves and F.S.Navarra, Phys.Lett.B**669** (2008)331.

13. G.Altarelli and G.Martinelli, Phys.Lett.B**76** (1978)89.

14. A.M.Cooper-Sarkar et al., Z.Phys.C**39** (1998)281.

15. G.R.Boroun and B.Rezaei, Eur. Phys. J. C**72** (2012)2221.

16. K.J.Eskola, V.J.Kolhinen and C.A.Salgado, Eur.Phys.J.C**9** (1999)61.

17. K.J.Eskola, H.Paukkunen and C.A.Salgado, JHEP**0807** (2008)102.

18. D.de Florian and R.Sassto, Phys.Rev.D**69** (2004)074028.

19. M.Hirai, S.Kumano and T.H.Nagai, Phys.Rev.C**76** (2007) 065207.

20. H.Paukkunen, K.J.Eskola and N.Armesto, arXiv:hep-ph/1306.2486(2013).

21.E.R.Cazaroto, F.Carvalho. V.P.Goncalves and F.S.Navarra, Phys.Lett.B**671** (2009)233.

22.X.Guo and J.Li, Nucl.Phys.A**783** (2007)587; K. Golec-Biernat et al., Nucl.Phys.B**527** (1998)289.

23. J.Qiu and I.Vitev, Phys.Rev.Lett.**93** (2004)262301; B.Kopeliovich et al., Phys.Rev.C **62** (2000)035204;

J.Raufeisen, arXiv:hep-ph/0204018 (2002).

TABLE IV: The same Table 2 with  $m_t$ .

$Q^2(GeV^2)$	$x_c^{A=1}$	$x_c^{A=12}$	$x_c^{A=208}$
2	0.81E-18	0.22E-16	0.99E-15
10	0.38E-17	0.10E-15	0.47E-14
100	0.20E-16	0.54E-15	0.24E-13

### Figure Captions

Fig.1.  $R_g$  and  $R_L$  evaluated as a function of  $x$  at  $Q^2 = 2, 10$  and  $100 GeV^2$  for nuclei  $A = 12$  and  $A = 208$  with the KLN model.

Fig.2.  $R_g$  and  $R_L$  evaluated as a function of the geometrical scalings at  $Q^2 = 2 GeV^2$  for nuclear  $A = 12$ .

Fig.3. The same Fig.2 for  $A = 208$ .

Fig.4. The ratio  $R_L^H = \frac{F_L^{H(A)}}{AF_L^{H(p)}}$  for  $A = 12$  at  $Q^2 = 2, 10$  and  $100 GeV^2$ .

Fig.5. The same Fig.4 for  $A = 208$ .

Fig.6. The nonlinear and shadowing behavior of  $R_L^H$  for  $A = 12$  in accordance with new geometrical transition point.

Fig.7. The same Fig.6 for  $A = 208$ .

Fig.8.  $R_L^{total}$  for  $A = 12$  and  $A = 208$  at  $Q^2 = 2 GeV^2$ .

TABLE III: The same Table 2 with  $m_b$ .

$Q^2(GeV^2)$	$x_c^{A=1}$	$x_c^{A=12}$	$x_c^{A=208}$
2	0.23E-10	0.64E-9	0.29E-7
10	0.22E-10	0.61E-9	0.27E-7
100	0.17E-12	0.48E-11	0.21E-9

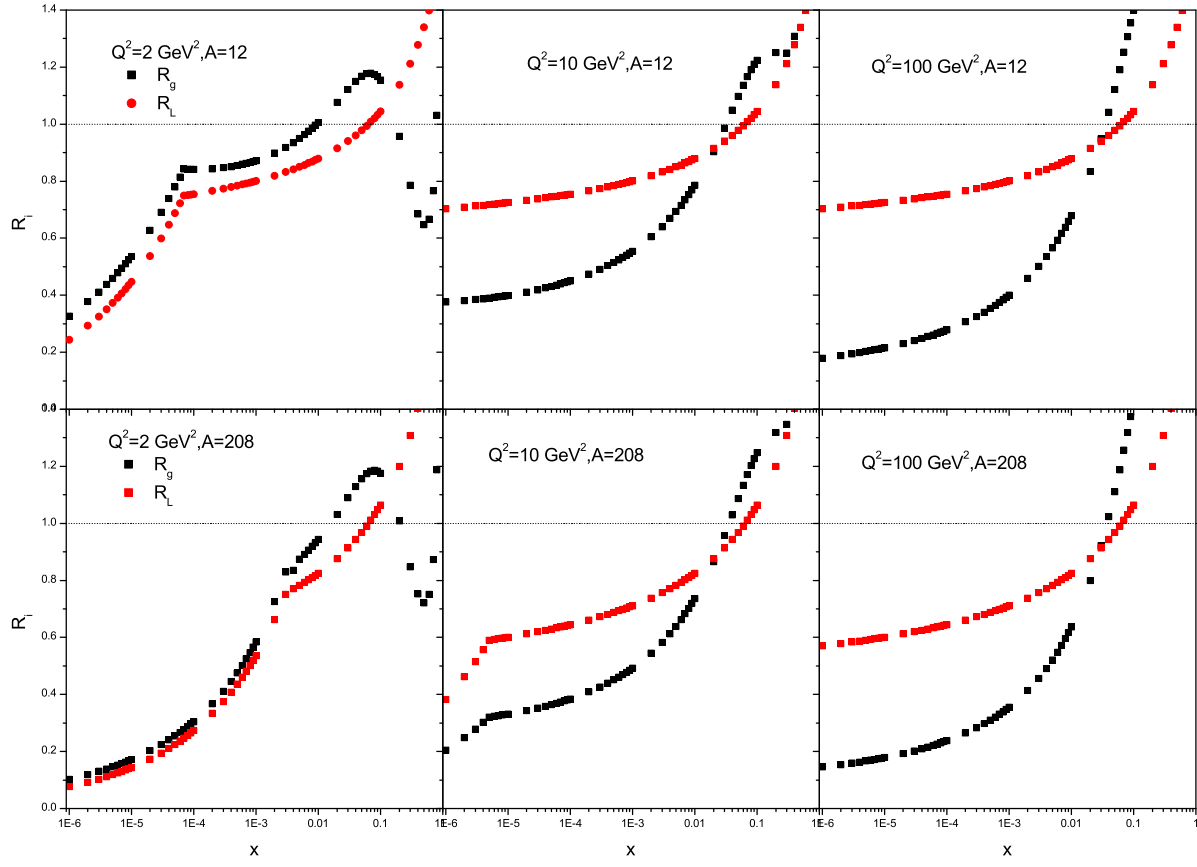


Fig.1

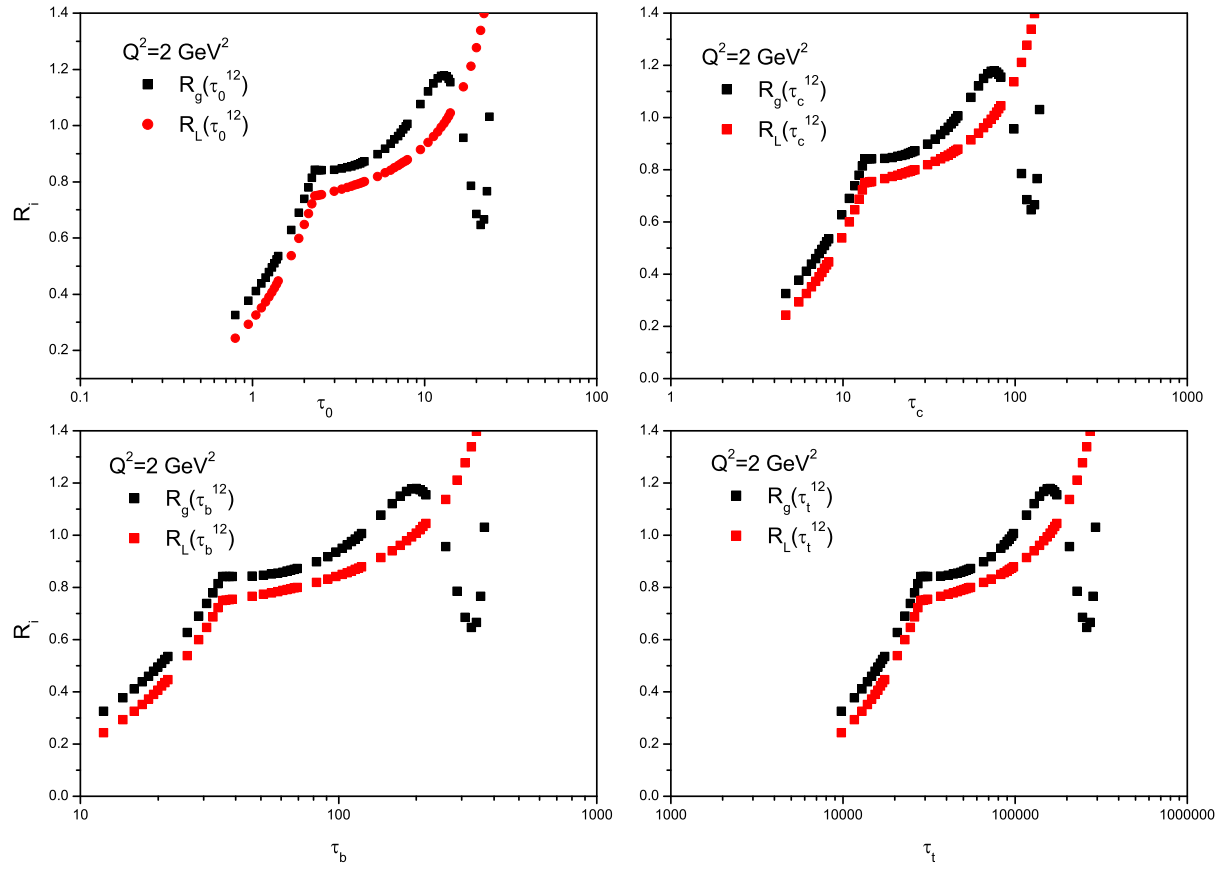


Fig.2

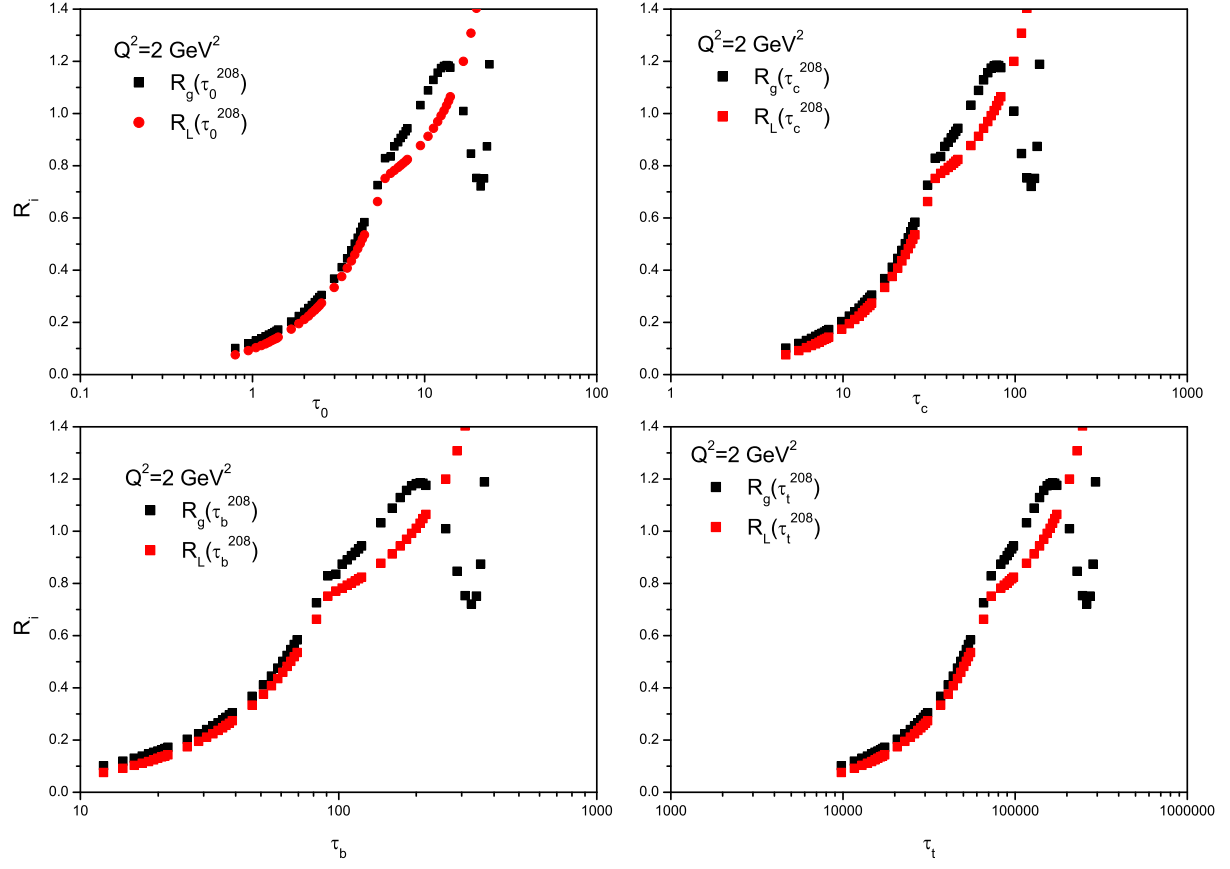


Fig.3



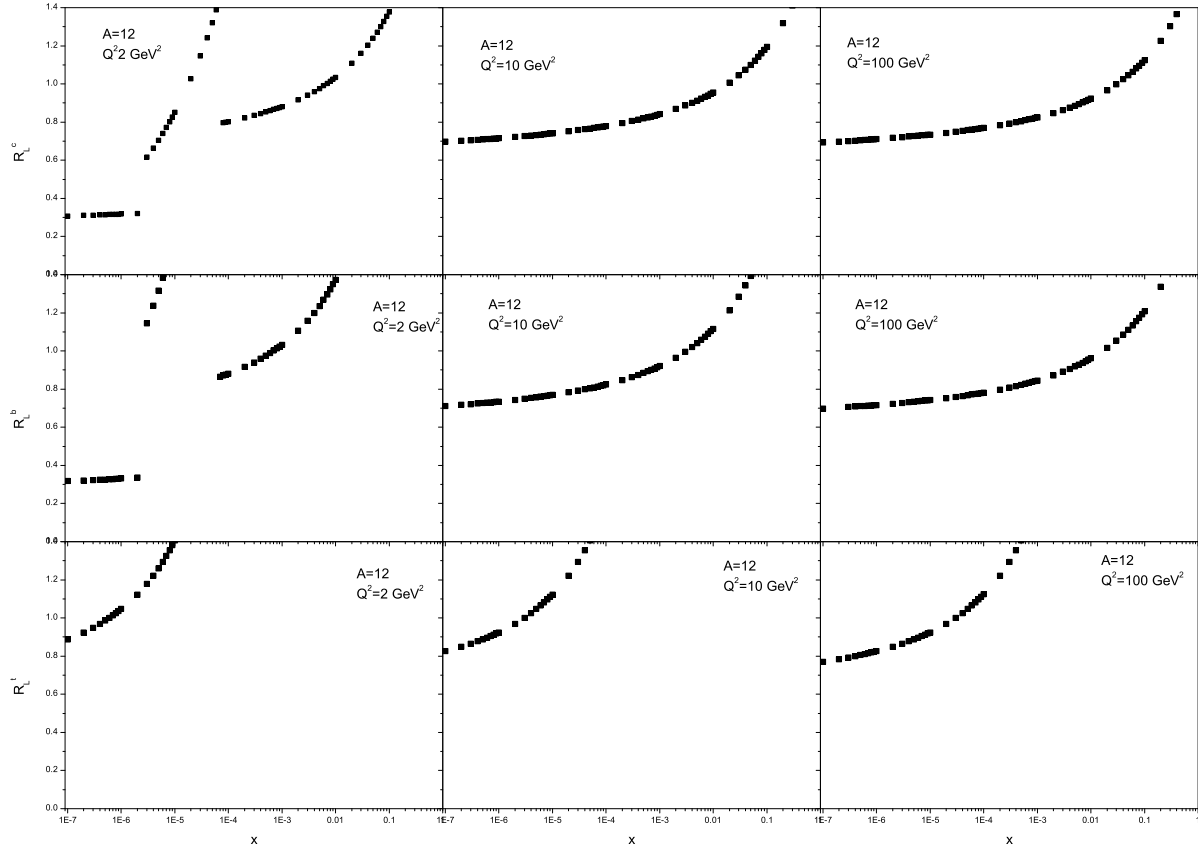


Fig.4

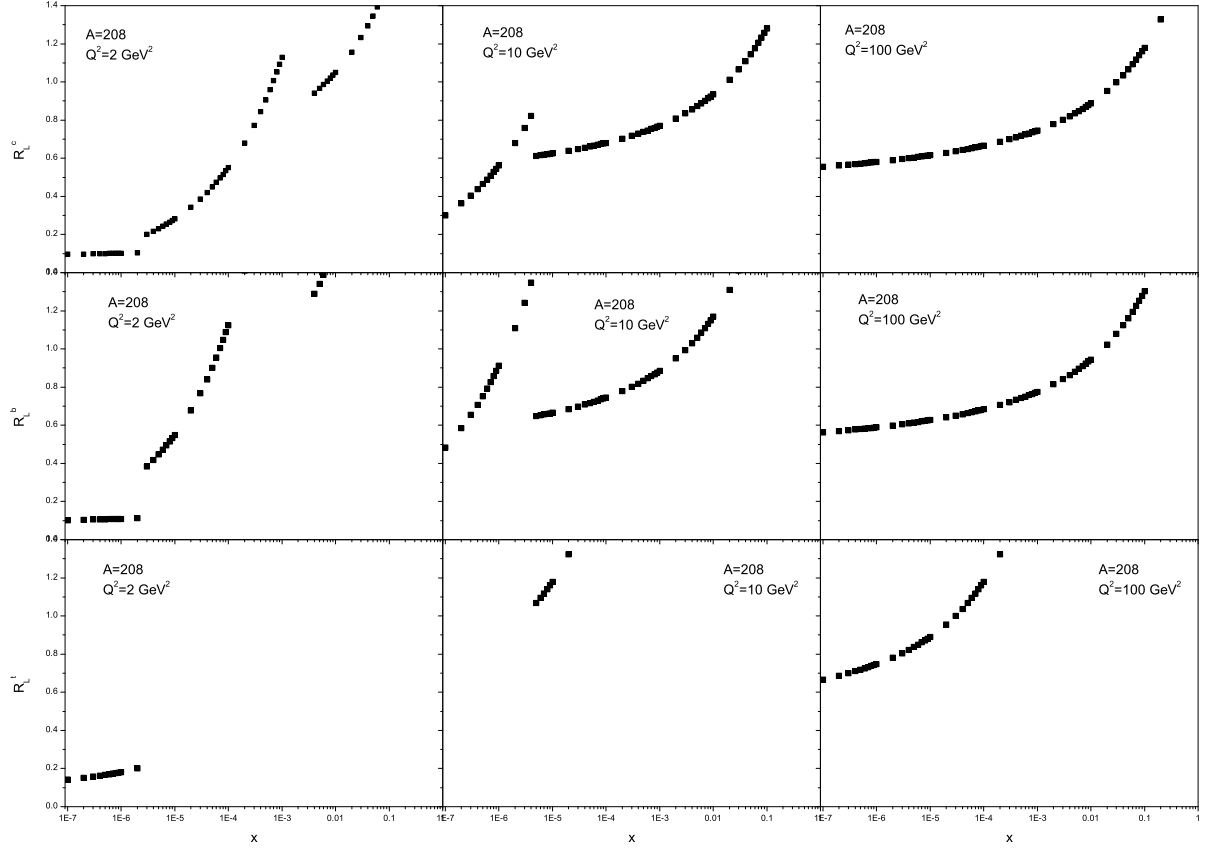


Fig.5

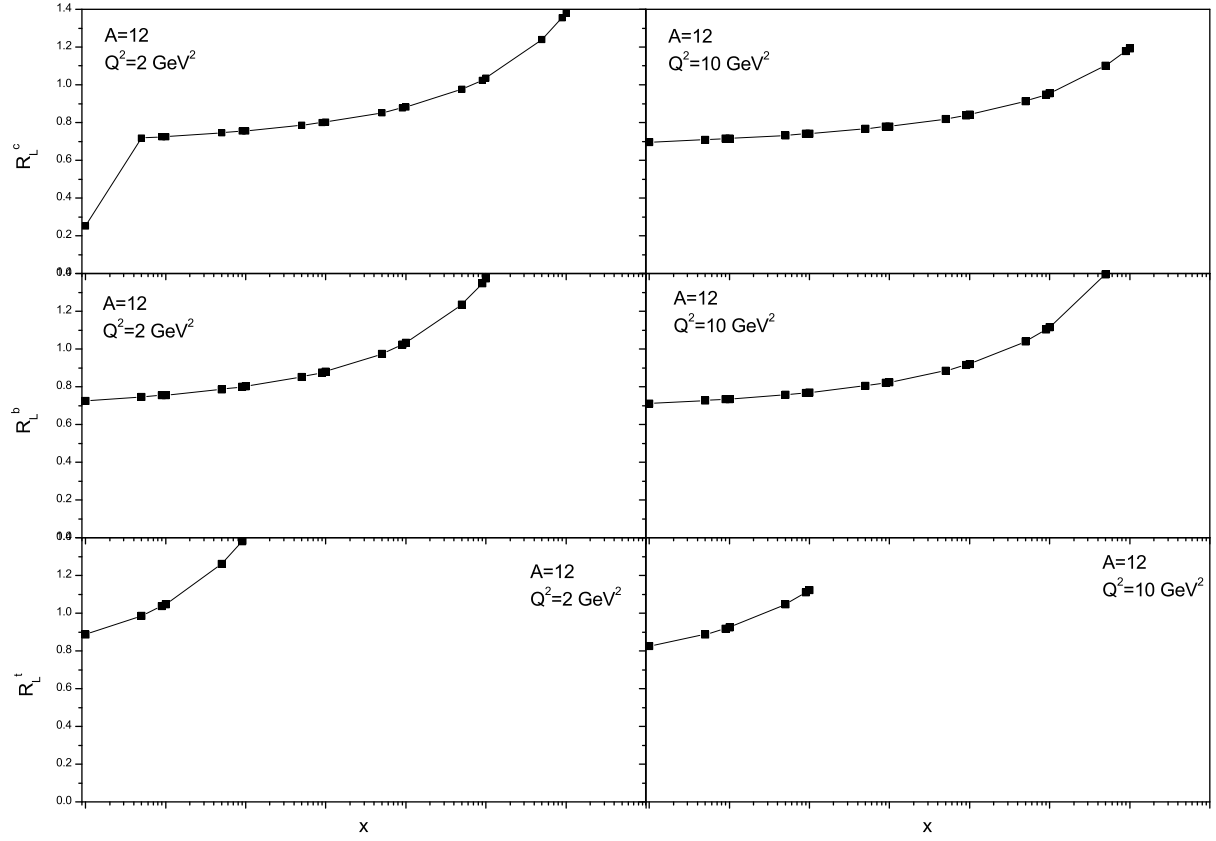


Fig.6

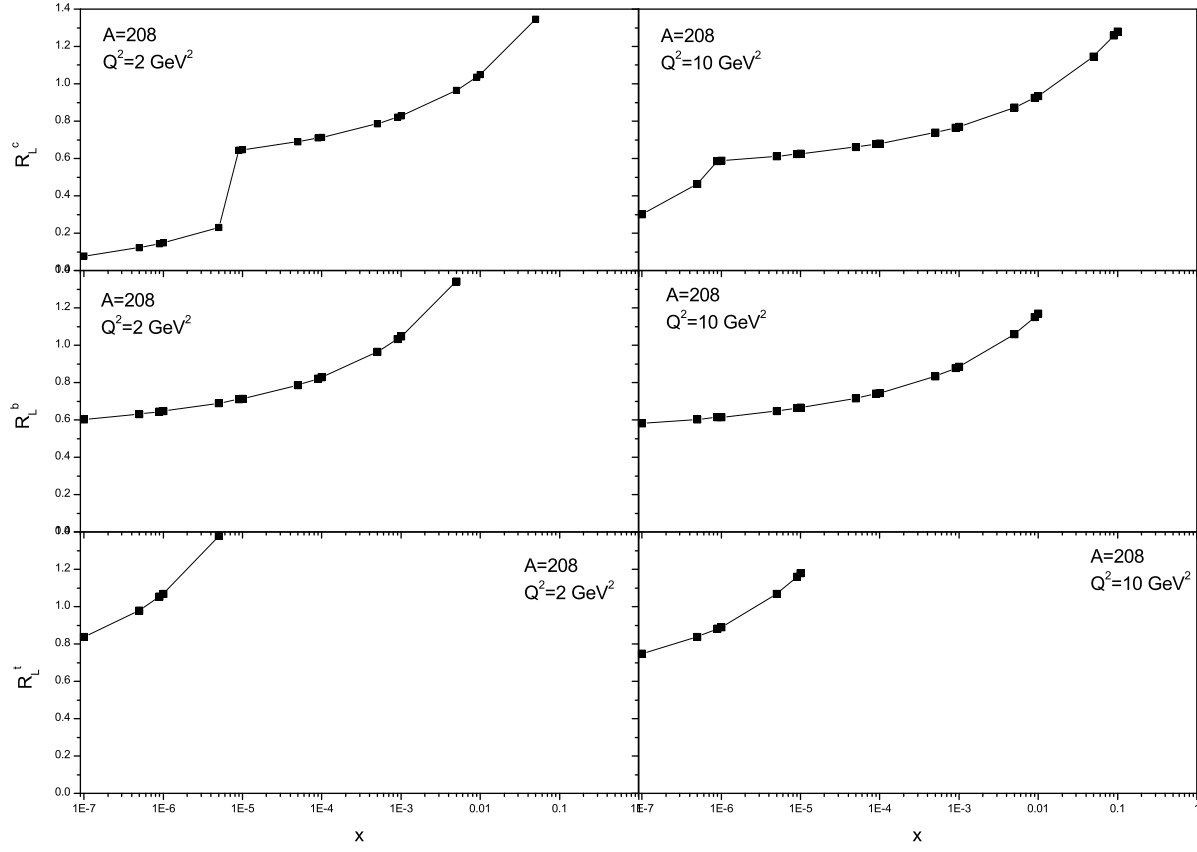


Fig.7

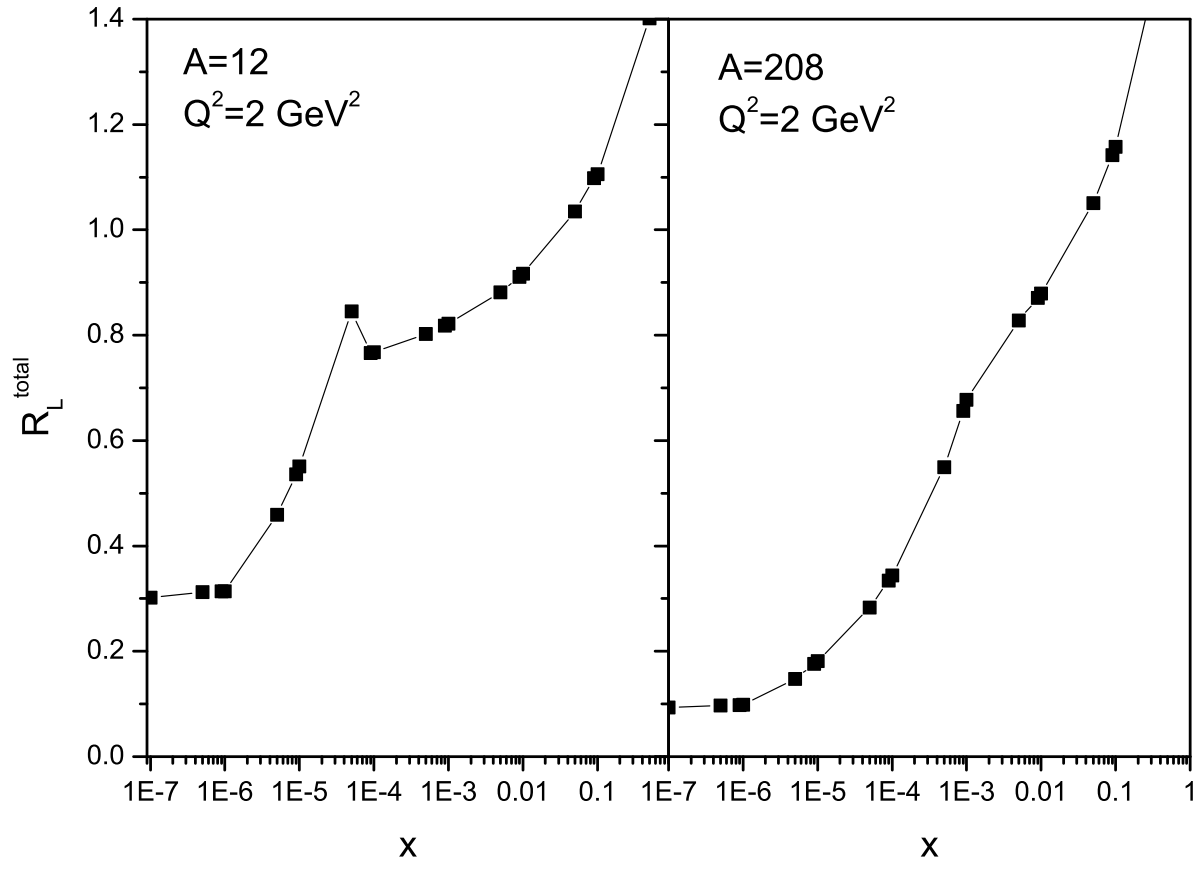


Fig.8